

## Luminescent properties of $\text{LaI}_3\text{-Ce}$ microcrystals embedded in NaI host

*A.S.Pushak*<sup>1</sup>, *V.V.Vistovskyi*<sup>2</sup>, *T.M.Demkiv*<sup>2</sup>, *Yu.R.Datsyuk*<sup>2</sup>,  
*I.M.Kravchuk*<sup>3</sup>, *L.T.Karplyuk*<sup>2</sup>, *A.V.Gektin*<sup>4</sup>, *A.S.Voloshinovskii*<sup>2</sup>

<sup>1</sup>Ukraine Academy of Printing, 19 Pidgolosko Str., 79020 Lviv, Ukraine

<sup>2</sup>I.Franko National University of Lviv,

8 Kyryla i Mefodiya Str., 79005 Lviv, Ukraine

<sup>3</sup>Lviv Polytechnic National University, 12 S.Bandery Str.,  
79000 Lviv, Ukraine

<sup>4</sup>Institute for Scintillation Materials, STC "Institute for Single Crystals",  
National Academy of Sciences of Ukraine, 60 Lenin Ave., 61001 Kharkiv,  
Ukraine

*Received June 08, 2015*

Luminescence-kinetic properties of  $\text{LaI}_3\text{-Ce}$  microcrystals of 1–10  $\mu\text{m}$  size in NaI– $\text{LaI}_3\text{-Ce}$  system are studied upon 2.5–12 eV excitation using synchrotron radiation. The luminescent properties of cerium centers in the embedded  $\text{LaI}_3\text{-Ce}$  microcrystals are revealed to be similar to those for the bulk  $\text{LaI}_3\text{-Ce}$  crystals. The mechanisms of cerium centers luminescence excitation in the NaI– $\text{LaI}_3\text{-Ce}$  crystalline system upon excitation in the transparency and fundamental absorption range of NaI and  $\text{LaI}_3$  matrixes and mechanisms of thermal quenching of cerium ions luminescence in the  $\text{LaI}_3$  microcrystals are discussed.

**Keywords:** luminescence quenching, luminescence decay kinetics,  $\text{LaI}_3\text{-Ce}$  microcrystals embedded in NaI host.

Исследованы спектрально-люминесцентные и люминесцентно-кинетические свойства микрокристаллов  $\text{LaI}_3\text{-Ce}$  размером 1–10 мкм, диспергированные в матрице NaI при синхротронном возбуждении в диапазоне энергий 2.5–12 эВ. Люминесцентные свойства цериевых центров в микрокристаллах  $\text{LaI}_3\text{-Ce}$  подобны их объемным аналогам. Обсуждаются механизмы возбуждения люминесценции цериевых центров в кристаллической системе NaI– $\text{LaI}_3$ (1%)– $\text{CeI}_3$ (0.05%) при возбуждении в области прозрачности и фундаментального поглощения матриц NaI и  $\text{LaI}_3$ , а также механизмы температурного тушения люминесценции ионов церия в микрокристаллах  $\text{LaI}_3$ .

**Люмінесцентні властивості мікрокристалів  $\text{LaI}_3\text{-Ce}$ , вкраплених у матрицю NaI.**  
*A.S.Пушак, В.В.Вістовський, Т.М.Демків, Ю.Р.Дацюк, І.М.Кравчук, Л.Т.Карплюк, О.В.Гектін, А.С.Волошиновський.*

Досліджено спектрально-люмінесцентні і люмінесцентно-кінетичні властивості мікрокристалів  $\text{LaI}_3\text{-Ce}$  розміром 1–10 мкм, вкраплені в матриці NaI при синхротронному збудженні в діапазоні енергій 2.5–12 еВ. Люмінесцентні властивості церієвих центрів у мікрокристалах  $\text{LaI}_3\text{-Ce}$  є подібні до їх об'ємних аналогів. Обговорюються механізми збудження люмінесценції церієвих центрів в кристалічній системі NaI– $\text{LaI}_3$ (1%)– $\text{CeI}_3$ (0.05%) при збудженні в області прозорості і фундаментального поглинання матриць NaI і  $\text{LaI}_3$ , та механізми температурного гасіння люмінесценції іонів церію у мікрокристалах  $\text{LaI}_3$ .

## 1. Introduction

$\text{LaX}_3$  ( $X = \text{Cl}, \text{Br}, \text{I}$ ) single crystals doped with  $\text{Ce}^{3+}$  ions attract the attention of researchers due to good scintillation properties: high density, significant light yield and energy resolution [1–5]. The scintillation properties of  $\text{LaX}_3\text{-Ce}$  crystals are known to be improved at changing the halide in the  $\text{Cl} \rightarrow \text{Br} \rightarrow \text{I}$  row [3, 6], however, for  $\text{LaI}_3\text{-Ce}$  crystal the luminescence of cerium centers occurs only at low temperatures [4] therefore it may be considered as potential cryogenic scintillator. From perspective of practical use of  $\text{LaX}_3\text{-Ce}$  crystals there are difficulties associated with their hygroscopicity and low symmetry of the crystalline lattice. Latter complicates the growth of large size crystals. Therefore the perspective way for studying and practical use of the highly hygroscopic  $\text{LaX}_3\text{-Ce}$  crystals is fabrication of embedded  $\text{LaX}_3\text{-Ce}$  microcrystals in a non-hygroscopic or less hygroscopic matrix of high crystalline symmetry [7–9]. One of the possible matrices is NaI crystal which is characterized by less hygroscopicity than  $\text{LaI}_3$ .

The micro- or nanocrystals embedded in dielectric matrix can be formed by aggregation processes of impurity ions. Such the impurity aggregation is already studied for a significant quantity of halide compound [7–13]. The after-growth temperature annealing of the doped crystal affects on efficiency of embedded micro- or nanocrystals formation. Chemical composition of the obtained embedded microcrystals can correspond either to the impurity molecule or to the complex compound in the case if impurity forms a compound with the matrix material. For example, activation of KCl crystal by  $\text{LaCl}_3$  leads to formation of  $\text{K}_2\text{LaCl}_5$  microcrystals in the KCl matrix [14]. At the same time, the adding of  $\text{LaX}_3$  impurities into the NaX crystal leads to effective formation of  $\text{LaX}_3$  ( $X = \text{Cl}, \text{Br}$ ) microcrystals [9, 15]. In this case, one can obtain the embedded La-containing microcrystals protected from atmospheric influences, which possess the scintillation properties corresponding to their bulk analogs. To obtain the  $\text{Ce}^{3+}$  ions doped microcrystals the  $\text{CeX}_3$  impurities are added to the initial mixture. Prevailing introducing of the impurity cerium ions in the embedded microcrystals instead of NaI matrix is due to the same valency and close ionic radii of cerium and lanthanum [9].

Fabrication of the high hygroscopic of  $\text{LaI}_3\text{-Ce}$  crystals embedded in NaI matrix al-

lows to prevent the influence of atmospheric moisture, to study more exactly luminescent parameters of  $\text{LaI}_3\text{-Ce}$  and mechanisms of excitation energy transfer from the NaI matrix to the dispersed  $\text{LaI}_3\text{-Ce}$  microcrystals. Hence, the spectral-kinetic luminescent properties of NaI- $\text{LaI}_3$ (1 mol.%)- $\text{CeI}_3$ (0.05 mol.%) system was studied in this work. Some results of this study are also reported in [16].

## 2. Experimental details

NaI- $\text{LaI}_3$ (1 mol.%)- $\text{CeI}_3$ (0.05 mol.%), NaI- $\text{LaI}_3$ (1 mol.%) and NaI- $\text{CeI}_3$ (0.1 mol.%) crystals were grown in evacuated quartz ampoules by the Bridgman-Stockbarger technique using a moving vertical ampoule. As-grown NaI- $\text{LaI}_3\text{-Ce}$  crystals were annealed at 200°C during 100 h for an activation of the impurity ions aggregation.

Measurements of the emission, luminescence excitation spectra and luminescence decay kinetics of the NaI- $\text{LaI}_3\text{-Ce}$  crystals were performed using the facility of SUPERLUMI station at HASYLAB (DESY, Hamburg) [17]. A cryostat with flowing helium was used to carry out low-temperature ( $T = 10$  K) measurements. The emission spectra were studied within the range of 200–800 nm with the spectral resolution of 1 nm using Action Research Corporation (ARC) "Spectra Pro 308" 30 cm monochromator-spectrograph equipped with Princeton Instruments CCD detector and HAMAMATSU R6358P photomultiplier. The luminescence excitation spectra were measured with the resolution of 4 Å within 2.5–12 eV by the means of primary 2 m monochromator in 15° McPearson mounting and secondary ARC monochromator.

Investigation of the crystal microstructure was carried out using a scanning electron microscope (SEM JEOL JSM-T220A) with an X-ray analyzer (dispersion Si(Li) detector). Micrographs were obtained using secondary electrons and cathodoluminescence registration modes.

## 3. Results and discussion

### 3.1. Scanning electron microscopy

Microcrystalline aggregates with the size in range from 1 to 10 μm on the freshly cleaved surface of NaI- $\text{LaI}_3\text{-Ce}$  crystalline system are observed on SEM micrographs (Fig. 1). Electron beam analysis has revealed the microcrystalline inclusion containing lanthanum and iodine ions in the ratio of 1:3, that corresponds to  $\text{LaI}_3$  com-

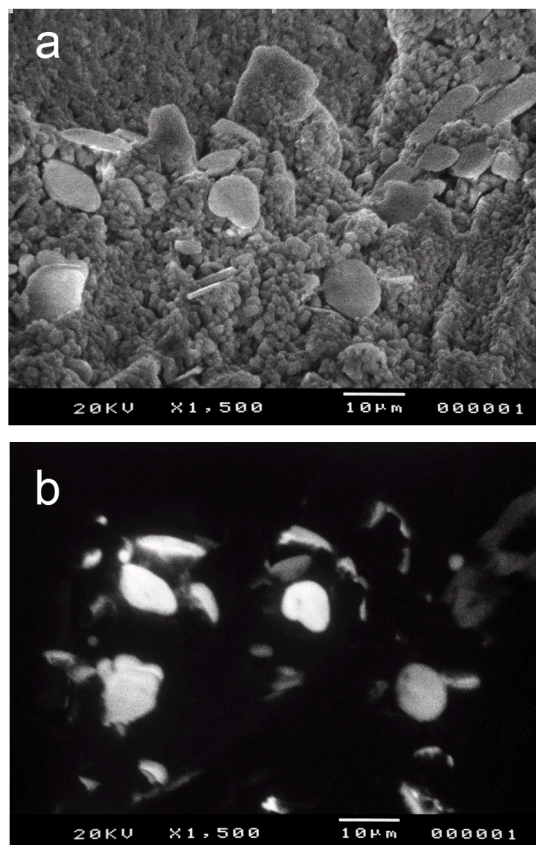


Fig. 1. Micrograph of NaI-Lal<sub>3</sub>-Ce freshly cleaved surface obtained by SEM in secondary electrons registration mode (a) and cathodoluminescence mode (b) at  $T = 295$  K.

pound. In cathodoluminescence registration mode of cleaved surface of NaI-Lal<sub>3</sub>-Ce crystal the Lal<sub>3</sub> microinclusions observed as bright spots (see Fig. 1b). Since the intrinsic luminescence of Lal<sub>3</sub> and NaI matrixes at the room temperature is weak the observed emission should be ascribed to luminescence of cerium ions only. The obtained micrograph indicates that the microinclusions contain majority of impurity Ce<sup>3+</sup> ions. Otherwise the luminescence of cerium ions in cathodoluminescence mode should be observed from the whole cleaved surface of the NaI-Lal<sub>3</sub>-Ce crystal. Using the electron beam analysis the presence of cerium ions of low concentration in the microinclusions was also found. Thus, based on the SEM studies of the cleaved surface of NaI-Lal<sub>3</sub>-Ce crystalline system it is possible to conclude that the Ce<sup>3+</sup>-doped Lal<sub>3</sub> microcrystals of 1–10 µm size is formed in the NaI-Lal<sub>3</sub>-Ce crystalline system and most of cerium ions are located within the microcrystals.

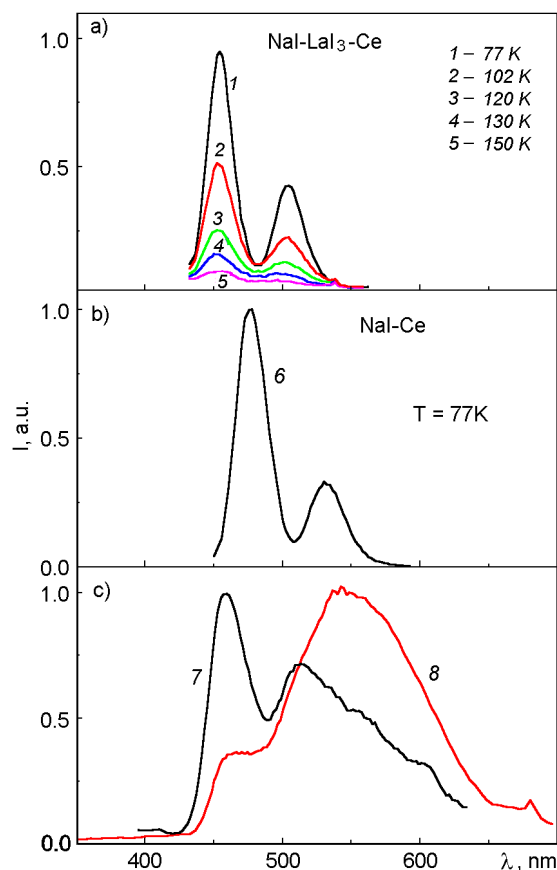


Fig. 2. Luminescence spectra of (a) — NaI-Lal<sub>3</sub>-Ce crystal at different temperatures: 1 — 77, 2 — 102, 3 — 120, 4 — 130, 5 — 149 K; (b) — NaI-Ce (curve 6) at  $T = 77$  K ( $\lambda_{exc} = 411$  nm); (c) — NaI-Lal<sub>3</sub>-Ce (curve 7,  $\lambda_{exc} = 323$  nm) and NaI-Lal<sub>3</sub>(1 mol.%) (curve 8,  $\lambda_{exc} = 300$  nm) crystals at  $T = 77$  K.

### 3.2. Emission and excitation spectra

Luminescence spectrum of the NaI-Lal<sub>3</sub>-Ce crystalline system upon excitation in the range of intracenter absorption of cerium ions (412 nm) measured at  $T = 77$  K consists of two bands peaked at 453 (2.74 eV) and 504 nm (2.46 eV) (Fig. 2a). Energy separation between these bands is 0.24 eV. The structure of the luminescence spectrum is characteristic for  $5d \rightarrow 4f$  luminescence of impurity Ce<sup>3+</sup> ions. Similar luminescence spectrum observed in [4] for the bulk Lal<sub>3</sub>-Ce crystal, where luminescence maxima of cerium ions are at 452 and 502 nm. Since  $5d \rightarrow 4f$  luminescence bands of cerium ions is very sensitive to the matrix crystal field, the spectral correlation of the luminescence bands for the NaI-Lal<sub>3</sub>-Ce crystal and bulk Lal<sub>3</sub>-Ce crystal indicates that 453

and 504 nm luminescence bands corresponds to emission of cerium ions in the  $\text{LaI}_3$  microcrystals embedded in the NaI matrix. The absence in the luminescence spectra of the NaI- $\text{LaI}_3$ -Ce crystalline system of luminescence bands peaked at 476 and 531 nm responsible for the emission of cerium ions in the NaI matrix (Fig. 2b, curve 6) indicates the efficient entry of cerium ions in the  $\text{LaI}_3$  microcrystals.

As temperature increases the intensity of the cerium ions luminescence in the  $\text{LaI}_3$  microcrystals sharply decreases (Fig. 2a) and at temperature of 150 K is more than ten times less than the intensity of cerium luminescence at 77 K. The same temperature behavior of the luminescence spectra of the  $\text{LaI}_3$ -Ce crystals is explained in [4] by the close location of excited cerium  $5d$ -state to the bottom of the conduction band of the  $\text{LaI}_3$  crystal. In the case of excitation of the NaI- $\text{LaI}_3$ -Ce crystalline system in the fundamental absorption range of the  $\text{LaI}_3$  crystal ( $\lambda_{exc} = 325$  nm (3.82 eV)) in addition to cerium luminescence bands the broad band peaked at 564 nm (2.2 eV) is observed (Fig. 2c, curve 7). This luminescence band is present also in the emission spectrum of the NaI- $\text{LaI}_3$  (1 mol.%) system obtained without doping by cerium ions (Fig. 2c, curve 8). In the bulk crystals of  $\text{LaI}_3$ -Ce [4] and other lanthanum halides the similar luminescence band is also observed [15, 18]. Since 564 nm luminescence band is observed in the case of excitation in the fundamental absorption range of the  $\text{LaI}_3$  microcrystals, one can suppose that it corresponds to the intrinsic luminescence of  $\text{LaI}_3$ .

Structure of the luminescence excitation spectrum of cerium centers for the NaI- $\text{LaI}_3$ -Ce crystal is complicated (Fig. 3). In the energy range of 2.6–3.4 eV the intracenter absorption bands of cerium ions are observed. These bands reflect the structure of the lowest excited  $5d$ -level of cerium ions split by the crystal field of  $\text{LaI}_3$  matrix. It is possible to clearly separate the intracenter absorption bands at 427 (2.90), 397 (3.12) and 377 (3.28 eV) nm. Other missing  $4f$ - $5d$  electronic transitions possibly can be masked by the band-to-band transitions. At higher excitation energies (3.6–5.0 eV) (Fig. 3, curve 1) the structure of cerium luminescence excitation spectrum is identical to that for intrinsic luminescence band of the  $\text{LaI}_3$  microcrystals (564 nm) (see Fig. 3, curve 3). This means that in the  $\text{LaI}_3$  microcrystals there is effective energy transfer from the matrix to cerium lumines-

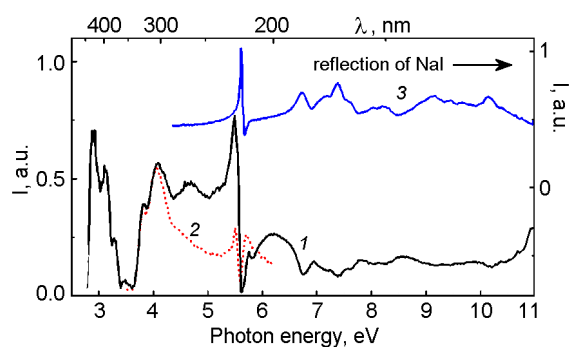


Fig. 3. Luminescence excitation spectra of  $\lambda_{em} = 503$  nm band (curve 1) and  $\lambda_{em} = 564$  nm (curve 2) of NaI- $\text{LaI}_3$ -Ce crystalline system at 77 K. Curve 3 — reflection spectrum of NaI.

cence centers. From these excitation spectra (Fig. 3, curves 1, 2) the fundamental absorption edge of the  $\text{LaI}_3$  microcrystals can be estimated as 3.6 eV. When luminescence of the NaI- $\text{LaI}_3$ -Ce crystal is excited by light quanta with energy more than ~5.0 eV, which match with the region of the fundamental absorption of the NaI matrix the structure of cerium luminescence excitation spectrum coincides with that for self-trapped exciton (STE) luminescence band of the NaI crystal ( $\lambda_{em} = 300$  nm) [19]. Since the STE luminescence of the NaI matrix overlaps with absorption of the  $\text{LaI}_3$ -Ce microcrystals one can assume that excitation energy transfer from the NaI matrix to embedded  $\text{LaI}_3$ -Ce microcrystals occurs through the reabsorption of the NaI STE emission by  $\text{LaI}_3$  matrix.

### 3.3. Temperature dependence of cerium luminescence parameters

To elucidate the type of temperature quenching of cerium luminescence centers in  $\text{LaI}_3$ -Ce microcrystals embedded in the NaI matrix the luminescence decay kinetics studies is of important. If the luminescence quenching occurs when the luminescent centers do not become excited, the luminescence intensity will decrease with increasing of temperature and luminescence decay kinetics will remain unchangeable. If the luminescence quenching is due to non-radiative decay of cerium ions from the excited state, in addition to decrease of luminescence intensity the shortening of luminescence decay kinetics constant should be observed. Temperature dependence of the cerium luminescence decay kinetics for the  $\text{LaI}_3$ -Ce microcrystals dispersed in the NaI matrix is shown in Fig. 4. The temperature

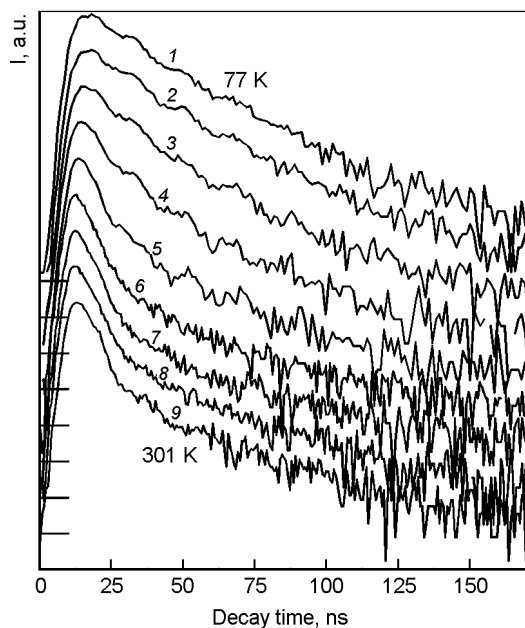


Fig. 4. Luminescence decay kinetics curves for cerium emission in NaI-Lal<sub>3</sub>-Ce crystalline system upon excitation in the range of intracenter absorption ( $E_{exc} = 2.91$  eV,  $E_{em} = 2.48$  eV) for different temperatures: 77; 81; 94; 116; 150; 177; 201; 260 and 301 K [16].

dependence of the luminescence intensity and decay time constants is compared in Fig. 5. The luminescence intensity decrease starts at the lower temperatures than the shortening of decay time constants. This indicates the existence of two mechanisms of luminescence quenching with different activation energies.

To find the activation energies for mentioned luminescence quenching mechanisms the experimental dependences of the intensity and decay time were approximated using the Mott formula:

$$I = \frac{I_0}{1 + A \exp(-\varepsilon/kT)},$$

where  $I$  — luminescence intensity at temperature  $T$ ,  $I_0$  — luminescence intensity at  $T = 0$  K,  $\varepsilon$  — activation energy of nonradiative transitions,  $k$  — the Boltzmann constant,  $A$  — the ratio of the radiative to nonradiative transitions rate at  $T = \infty$ . The similar formula was used for analysis of decay curves, only decay time constants  $\tau$  and  $\tau_0$  ( $\tau$  — decay time constant at temperature  $T$ ,  $\tau_0$  — decay time constant when quenching is absent) substitute  $I$  and  $I_0$ . Determined values of activation energy of the nonradiative transitions are 59 and

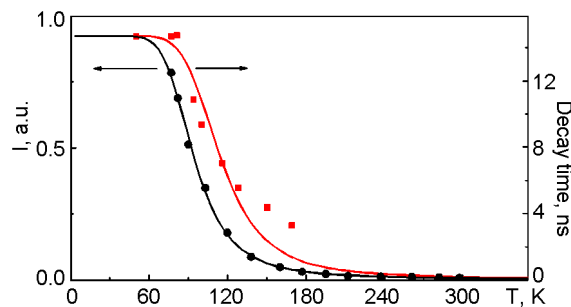


Fig. 5. Temperature dependences of cerium luminescence (circles) intensity and its decay time (rectangles) and fitting curves by the Mott formula (solid curves) [16].

70 meV for the temperature dependence of the intensity and decay time, respectively. The similar difference for activation energies also was reported in [4]. The difference in quenching activation energies determined from the temperature dependence of the luminescence intensity and decay time constants indicates that there are two ways for luminescence quenching. One of these mechanisms may be associated with transition of electrons from the excited  $5d$ -state of  $Ce^{3+}$  ion to the conduction band. Temperature activation of such transitions leads to reducing of luminescence intensity and the shortening of the decay time constant. However, in our case the temperature quenching of the luminescence intensity begins at  $\sim 18$  K lower than shortening of luminescence decay time constant (Fig. 5). To explain this fact one can assume that there is also another quenching mechanism associated with the electronic transitions from the ground  $4f$ -state of the cerium ion to the conduction band of Lal<sub>3</sub>. In this case the absorption of excitation quanta does not lead to the excitation of cerium ions and therefore there is the decrease of luminescence intensity without shortening of the decay time constant.

#### 4. Conclusions

Lal<sub>3</sub>-Ce microcrystals of 1–10  $\mu\text{m}$  size embedded in NaI matrix are revealed in NaI-Lal<sub>3</sub>-Ce crystalline system by means SEM and luminescence studies. Emission spectra upon the intracenter excitation show that most of cerium ions centers enter into the embedded microcrystals. The spectral positions of  $Ce^{3+}$  emission bands of the Lal<sub>3</sub>-Ce microcrystals embedded in the NaI

matrix coincide with that for the bulk  $\text{LaI}_3\text{-Ce}$  crystals. The cerium luminescence excitation spectrum of the  $\text{NaI-Lal}_3\text{-Ce}$  crystalline system reveals efficient excitation in the range of: (i) intracenter absorption of  $\text{Ce}^{3+}$  ion in 2.6–3.4 eV energy range; (ii) fundamental absorption of  $\text{LaI}_3$  (3.6–5.0 eV) that indicates the energy transfer from STE of  $\text{LaI}_3$  to  $\text{Ce}^{3+}$  ions; (iii) fundamental absorption of  $\text{NaI}$  ( $h\nu > 5$  eV). In the last case the energy transfer from the  $\text{NaI}$  matrix to embedded  $\text{LaI}_3\text{-Ce}$  microcrystals is due to the overlapping of STE emission of  $\text{NaI}$  with the fundamental absorption band of  $\text{LaI}_3$ .

The cerium emission in the embedded  $\text{LaI}_3\text{-Ce}$  microcrystals undergoes the strong temperature quenching as well as in the bulk  $\text{LaI}_3\text{-Ce}$  crystals. Two mechanisms of cerium emission quenching associated with the temperature stimulated electronic transitions into conduction band from ground  $4f$  and excited  $5d$ -levels are proposed.

The intrinsic luminescence band of the  $\text{LaI}_3$  microcrystals is revealed at 564 nm. The fundamental absorption edge of the  $\text{LaI}_3\text{-Ce}$  microcrystals is estimated as 3.6 eV.

The formation of the embedded microcrystals in low hygroscopic matrixes simplifies the investigation of strongly hygroscopic luminescence materials and allows the obtaining of composite materials with the new properties.

*Acknowledgments.* The authors would like to thank Dr.A.Kotlov for the support in the SUPERLUMI experiments.

### References

1. E.V.D.van Loef, P.Dorenbos, C.W.E.van Eijk et al., *Appl. Phys. Lett.*, **77**, 1467 (2000).
2. E.V.D.van Loef, P.Dorenbos, C.W.E.van Eijk et al., *Appl. Phys. Lett.*, **79**, 1573 (2001).
3. E.V.D.van Loef, P.Dorenbos, C.W.E.van Eijk et al., *Nucl. Instrum. Meth. Phys. Res. A*, **486**, 254 (2002).
4. A.Bessiere, P.Dorenbos, C.W.E.van Eijka et al., *Nucl. Instrum. Meth. Phys. Res. A*, **537**, 22 (2005).
5. K.W.Kramer, P.Dorenbos, H.U.Gudel et al., *J. Mater. Chem.*, **16**, 2773 (2006).
6. K.S.Shah, J.Glodo, M.Klugerman et al., *Nucl. Instrum. Meth. Phys. Res. A*, **505**, 76 (2003).
7. A.S.Pushak, V.V.Vistovskyy, S.V.Myagkota et al., *Functional Materials*, **17**, 294 (2010).
8. A.S.Pushak, P.V.Savchyn, V.V.Vistovskyy et al., *J. Luminescence*, **135**, 1 (2013).
9. V.V.Vistovskii, A.S.Pushak, S.V.Myagkota et al., *Optics Spectrosc.*, **109**, 352 (2010).
10. A.Voloshinovskii, A.Gloskovsky, S.Zazubovich et al., *Phys. Stat. Sol. B*, **225**, 257 (2001).
11. A.S.Pushak, V.V.Vistovskyy, T.M.Demkiv et al., *Optics Spectrosc.*, **117**, 593 (2014).
12. A.S.Pushak, V.V.Vistovskyy, A.S.Voloshinovskii et al., *Rad. Meas.*, **56**, 402 (2013).
13. A.S.Pushak, V.V.Vistovskyy, A.Kotlov et al., *Functional Materials*, **20**, 279 (2013).
14. A.S.Voloshinovskii, G.B.Stryganyuk, G.Zimmerer et al., *Phys. Stat. Sol. A*, **202**, R101 (2005).
15. V.V.Vistovskyy, P.V.Savchyn, G.B.Stryganyuk et al., *J. Phys.: Condens. Matter.*, **20**, 325218 (2008).
16. V.Vistovskyy, G.Stryganyuk, M.Pidzyrilo, A.Voloshinovskii, O.Antonyak, I.Pashuk, HASYLAB Annual Report (2007) 685.
17. G.Zimmerer, *Radiat. Meas.*, **42**, 859 (2007).
18. P.Dorenbos, E.V.D.van Loef, A.P.Vink et al., *J. Luminescence*, **117**, 147 (2006).
19. R.T.Williams, K.S.Song, *J. Phys. Chem. Solids*, **51**, 679 (1990).